https://ntrs.nasa.gov/search.jsp?R=19720016396 2020-03-23T13:09:19+00:00Z

2

(NASA-CR-126623) NONGASSING NICKEL-CADMIUM BATTERY ELECTRODES AND CELLS Quarterly Report, 15 Sep. - 15 Dec. 1971 E. Luksha, et al (Gould, Inc., Mendota Heights, Minn.) 18 Feb. 1972 44 p

N72-24046

Unclas
CSCL 10C G3/03 28185

NON-GASSING NICKEL-CADMIUM BATTERY ELECTRODES AND CELLS

DRA

Report No.: 712-122-2

Second Quarterly Report
15 September 1971 to 15 December 1971

Prepared by E. Luksha and D.J. Gordy Approved by C.J. Menard

18 February 1972

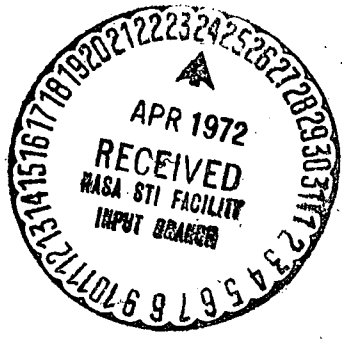

Jet Propulsion Laboratory
Contract No. 953184

Gould Inc., Gould Laboratories
Energy Technology
1110 Highway 110
Mendota Heights, Minnesota 55118

Reproduced by
NATIONAL TECHNICAL
INFORMATION SERVICE
U S Department of Commerce
Springfield VA 22151

NON-GASSING NICKEL-CADMIUM BATTERY ELECTRODES AND CELLS

Report No.: 712-122-2

Second Quarterly Report
15 September 1971 to 15 December 1971

Prepared by E. Luksha and D.J. Gordy Approved by C.J. Menard

18 February 1972

Jet Propulsion Laboratory
Contract No. 953184

Gould Inc., Gould Laboratories
Energy Technology
1110 Highway 110
Mendota Heights, Minnesota 55118

"This work was performed for the Jet Propulsion Laboratory, California Institute of Technology, as sponsored by the National Aeronautics and Space Administration under Contract NAS7-100."

"This report contains information prepared by Gould Inc., Gould Laboratories, Energy Technology, under JPL subcontract. Its content is not necessarily endorsed by the Jet Propulsion Laboratory, California Institute of Technology, or the National Aeronautics and Space Administration."

ABSTRACT

Supposedly long-lived nickel-cadmium batteries often fail due to severe gassing on charge. In order to increase the lives of such cells attempts are being made to construct "nongassing" positive and negative electrodes. The gassing characteristics of nickel electrodes were evaluated as a function of their loading, charge rate, and charge temperature. An analysis of the effects of each of these variables suggested that nickel electrodes with loading of 20 g/in.^{3} $Ni(OH)_2$ would be suitable for negative limited cells with a positive to negative capacity ratio of at least 1.7:1.

TABLE OF CONTENTS

LIST OF ILLUSTRATIONS

LIST OF TABLES

I. SUMMARY

There are various special applications for very long-lived, a decade or more, sealed nickel-cadmium batteries. The gassing which normally occurs in such cells limits their lives severely and in many cases is the sole cause of failure. An approach toward dramatically increasing their lives is to incorporate electrodes in these batteries that exhibit little or no gassing with controlled charge input.

This requires that: 1) the ratio of positive to negative active material ratio be changed to make cells negative limited, and 2) use materials that possess the highest possible overpotentials for the hydrogen evolution reaction so that the onset of hydrogen gassing would result in a large voltage step to be used to cut off the charge.

This report describes work conducted during the second quarter towards this end. Nickel electrodes at three different loading levels were characterized. Their gassing characteristics as a function of charge rate, temperature, and $Ni(OH)_2$ loading, at two stages, the third and twentieth cycle, in their lives was determined. It was found that there was no overall deterioration in the gassing characteristics after 20 cycles. The charge temperature was observed to be the single most important variable as far as gassing was concerned.

Higher loadings were found to promote gassing at lower states-of-charge. Further, high charge rates caused more severe gassing than low charge rates. A nickel electrode with a loading of about 20 g/in.^{3} $Ni(OH)_2$ was selected for use in negative limited cell with a positive to negative capacity ratio of at least 1.7:1.

II. INTRODUCTION

There is presently a need for very reliable and very long lived, about one decade, secondary batteries for applications such as in deep probe space vehicles, medical implantations, various cordless appliances, and other special uses. Sealed nickel-cadmium batteries are uniquely suited for such applications, mainly because of their long lives. However, the gassing that normally occurs in these cells, limits their reliability for very long life. The gassing problem becomes particularly severe during latter stages of the cell life. Aging effects on both electrodes can result in a set of circumstances that sealed cells can rupture due to hydrogen generation on charge. In many cases, gas evolution is the sole cause of life limitation of nickel-cadmium cells. As a result, an approach toward increasing the life of nickel-cadmium cells toward the decade or so required, is to construct cells designed with little or no gassing. The Jet Propulsion Laboratories have suggested an approach leading to the development of a "nongassing" nickel-cadmium battery. Their approach involves essentially three changes in the design of conventional nickel-cadmium batteries. These are:

1. Change the ratio of positive to negative active material in the cells so that the cells become negative limited.
2. Use a grid material for the cadmium electrode that has a high overpotential for the hydrogen evolution reaction so that the onset of hydrogen gassing would be signaled by a relatively large voltage step.
3. Incorporation of a miniature electronic charge control device that will be used externally to each cell to end the charge using the voltage step as a signal.

Gould Inc., Energy Technology Laboratories, under subcontract to JPL is involved in the design, development, and testing of a "nongassing" battery in accordance with parts 1 and 2 above.

To reach these goals, cadmium electrodes with the highest possible overpotential for the hydrogen evolution reaction are being developed. Five configurations were suggested by Gould as holding forth the most promise. These are:

1. An electrodeposited cadmium active mass on an expanded cadmium metal screen.
2. A cadmium active mass deposited in a porous silver substrate of precisely controlled porosity and pore-size.
3. An electrodeposited cadmium active mass on an expanded silver screen.

4. A pressed cadmium electrode prepared from electrolytic $Ch(OH)_2$ admixed with gold or silver powder.

5. Other novel materials with high overpotential for H_2 evolution reaction.

These various configurations are to be tested to determine the optimum configuration for minimum gassing as a function of temperature, charge and discharge rates, and loading. In addition, the program includes the determination of the gassing characteristics and specific capacities of state-of-the-art nickel electrode in order that the best nickel electrode from gassing and energy density considerations be employed for the proposed nongassing cell. A 3^3 full factorial experimental design is being employed for the collection of the above-mentioned data.

III. RESULTS AND DISCUSSION

A. Nickel Electrode Development

1. Electrode Characterization

In order to meet the program goals, one must have available design data on the gassing characteristics of the nickel electrode so that oxygen evolution on charge can be minimized or eliminated. There is little information available regarding the gas-free capacity of practical nickel electrodes as a function of their loading, and charge rate, and temperature. It is in this area of positive electrode gassing, that much of the work during the second quarter of this program was spent. The question that had to be answered was, since the cell is negative limited, what is the excess capacity required in the positive electrode to minimize oxygen evolution on charge? This would have to apply at the worst possible operating condition.

During the second quarter of the program, work was almost exclusively concerned with the testing of positive electrodes. This was required in order to obtain a design point around which to base a selection of hardware to meet the cell delivery requirement in the program. The preparation of the positive electrode plaques was described in the first quarterly report.

Electrodes impregnated at three different loading levels, 8.03 ± 0.33, 21.47 ± 0.66, and 31.63 ± 0.98 g/in.^{3} $Ni(OH)_2$ were characterized. The positive electrodes were assembled into cells in a positive limited configuration as previously described in the first quarterly report, and their gassing characteristics as a function of charge rate, temperature, and $Ni(OH)_2$ loading, at two stages, the third and twentieth cycle, in their lives was determined. The evolved gas or gasses were flushed from the cells with a carrier gas into a Beckman GC-2A gas chromatograph equipped with a differential thermal conductivity detector in a test installation which was also previously described. The use of the gas chromatograph permitted us to analyze the components of the effluent gas stream which together with a knowledge of the total gas flow rates, permitted quantitative determination of minute quantities of gasses evolved. These tests were performed employing a full factorial experimental design which is shown in Table 1. The charge temperature and the nickel electrode loadings are realistic levels of the variables. The charge rate is an experimental expedient which permits logging considerable cycle data in a short time, and yet providing useful design information. The experiments at the median temperature, 25°C, circled in the table, were not performed as yet. An analysis of the gassing data obtained at the two extreme temperatures, 20° and 50°C, showed that gassing characteristics were defined well enough at the experimental conditions chosen that obtaining additional data would serve no good purpose. Typical examples of good quality, complete gas evolution data is given in Figures 1 and 2. This data is for heavily loaded electrodes, 31.6 g/in.^{3} $Ni(OH)_2$, charged at the high current density 0.3 A/in.^{2} at the high and low temperature, respectively. The ordinate axis in these curves is the logarithm of O_2 volume generated. The very bottom of the axis is linear

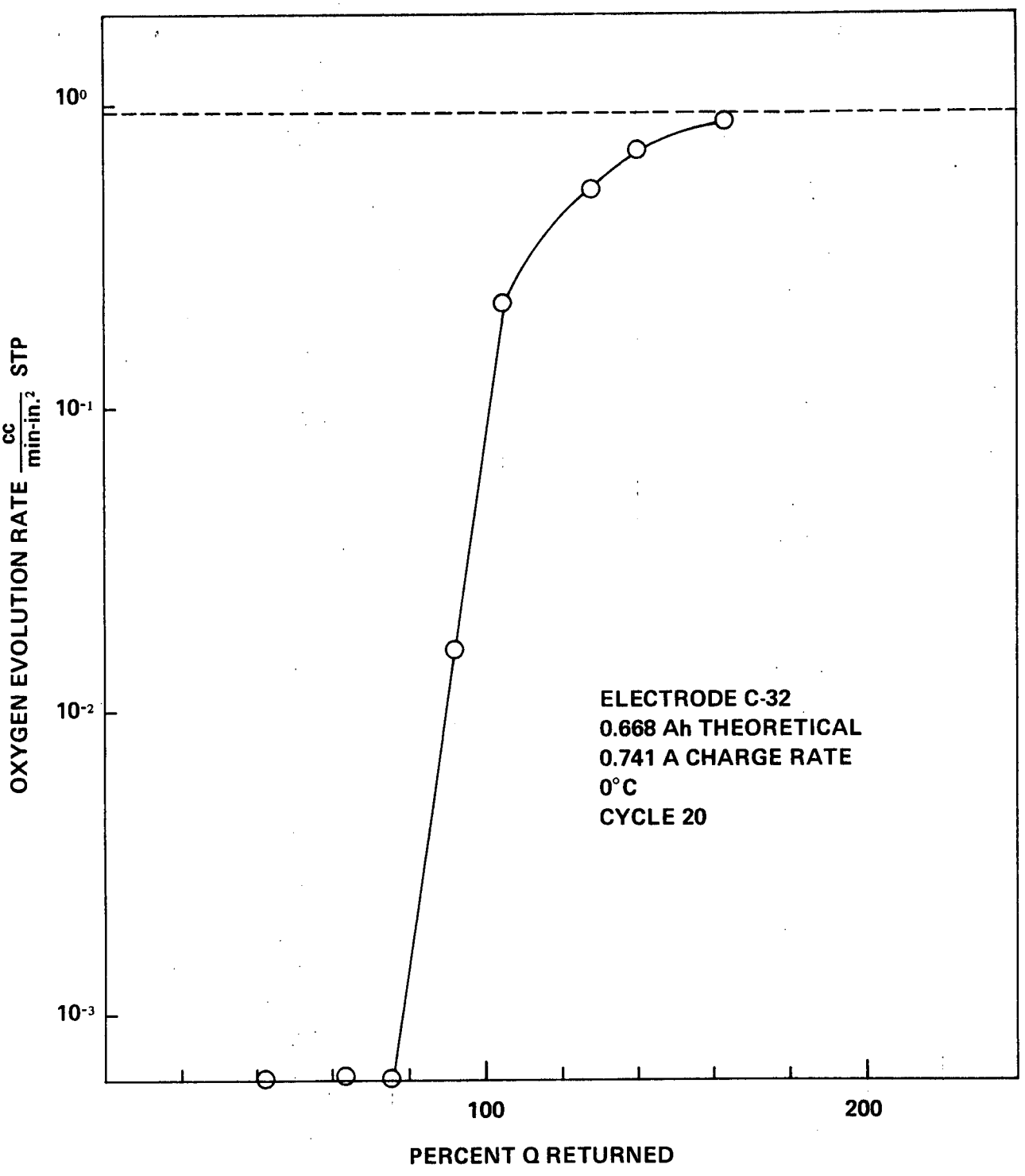

FIGURE 1. OXYGEN EVOLUTION ON CHARGE OF A HEAVILY LOADED NICKEL ELECTRODE

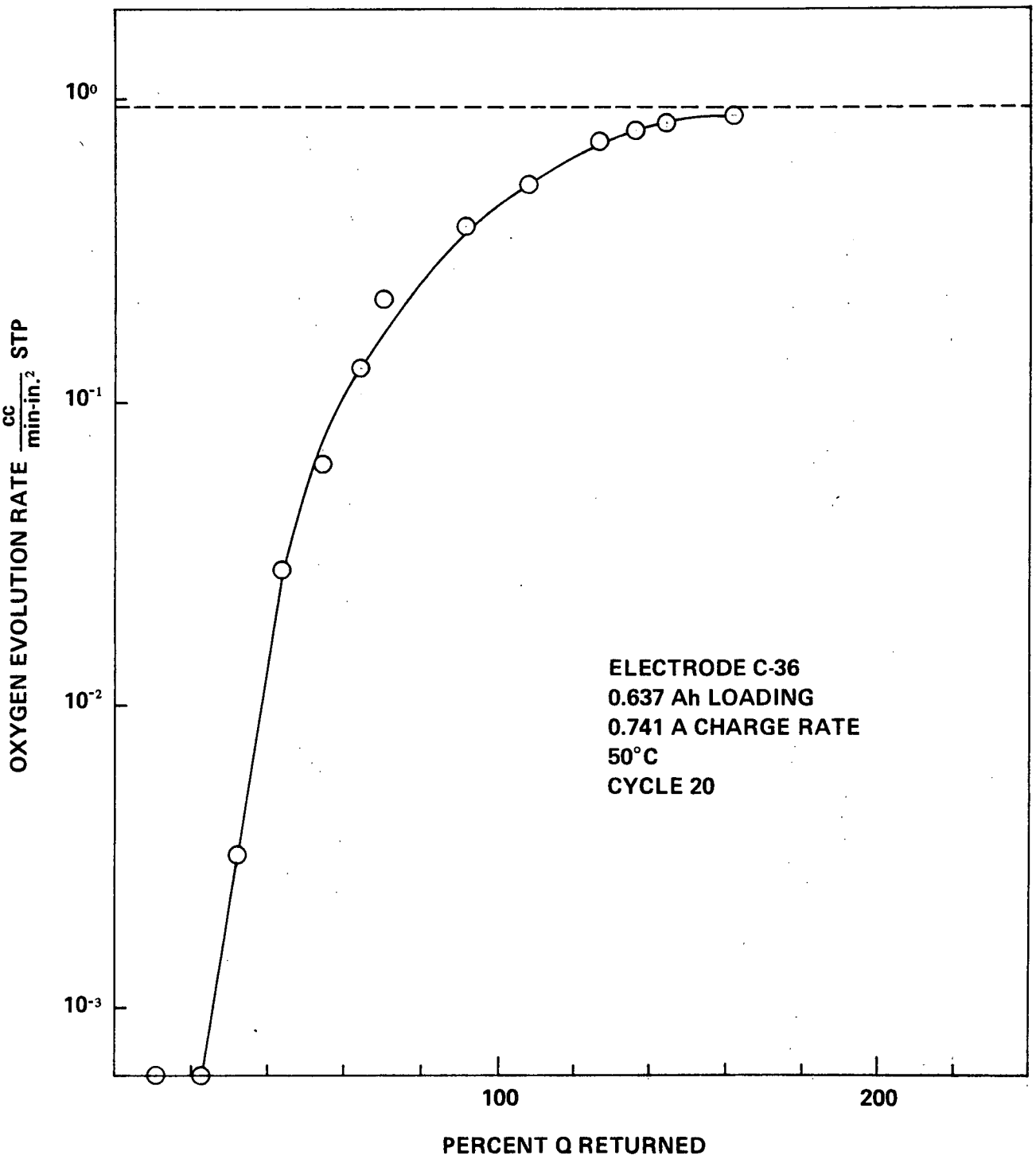

FIGURE 2. OXYGEN EVOLUTION ON CHARGE OF A HEAVILY LOADED NICKEL ELECTRODE

TABLE 1. EXPERIMENTAL DESIGN FOR STUDY OF POSITIVE ELECTRODE GASSING

Experimental Parameters and Limits for $Ni(OH)_2$ Electrode Gassing Study

		LEVELS		
		+	0	–
X_1	Charge Temperature, °C	50°	25°	0°
X_2	Charge Current Density, A/in.^{2}	0.27	0.18	0.09
X_3	Nickel Electrode Loading, g/in.^{3}	32.8	20.5	8.2

3^3 Full Factorial Experiment for Study of Nickel Electrode Gassing

EXP NO.	X_1	X_2	X_3	EXP NO.	X_1	X_2	X_3
1	+	+	+	15	–	0	0
(2)	0	+	+	16	+	–	0
3	–	+	+	(17)	0	–	0
4	+	0	+	18	–	–	0
(5)	0	0	+	19	+	+	–
6	–	0	+	(20)	0	+	–
7	+	–	+	21	–	+	–
(8)	0	–	+	22	+	0	–
9	–	–	+	(23)	0	0	–
10	+	+	0	24	–	0	–
(11)	0	+	0	25	+	–	–
12	–	+	0	(26)	0	–	–
13	+	0	0	27	–	–	–
(14)	0	0	0				

and zero is shown to account for the state of charge at which no oxygen evolution was detected. Rather abrupt changes from the gassing to the nongassing mode of operation is evident in these two figures. The dotted lines in these two figures represent the theoretical values of oxygen evolution for the current density in question. The oxygen evolution rate is seen to approach this value asymptotically. Perhaps a view offering a little better perspective is offered in Figures 3 and 4 in which essentially the same data is plotted but this time the ordinate axis is the percentage of the input charge current that is utilized for oxygen generation. This value was calculated from the total gas flow rates and the measured oxygen concentration in the gas stream. The abscissa is the fraction of charge returned that was removed during the previous cycle. The intersection of these curves with the line $X = 10\%$ was arbitrarily chosen as the "onset" of significant oxygen evolution, and of course is in reality the fraction of charge returned at which 10% of the current goes to oxygen evolution. From Figures 3 and 4 and 15 other sets of similar data, which are given in tabular form in Appendix A, Table 2 was constructed giving gassing data for both the third and twentieth cycles.

The values in Table 2 were used to calculate the average effect of each variable. This is determined by averaging over the levels of the remaining factors. The equation for such a calculation is:

$$E_j = \frac{1}{2} \cdot \frac{1}{N/3} \sum_{i=1}^{N} (Y_i)\,(C_{ij})$$

where:

- N is the number of tests performed
- i is the row position of the design
- j is the column position of the variable of the design
- Y is the test value recorded
- C is the multiplier value in the design.

The multipliers are given in Table 3.

The average effects of variable interactions was determined similarly from the following relation:

$$E_{jj_1} = \frac{1}{2} \cdot \frac{1}{N/3} \sum_{i=1}^{N} (Y_i)\,(C_{ij}C_{ij_1})$$

where as before, j is the column position of one variable and j_1 is the column position of the other variable.

The results of such computations are given in Table 4 for both the third and twentieth cycle.

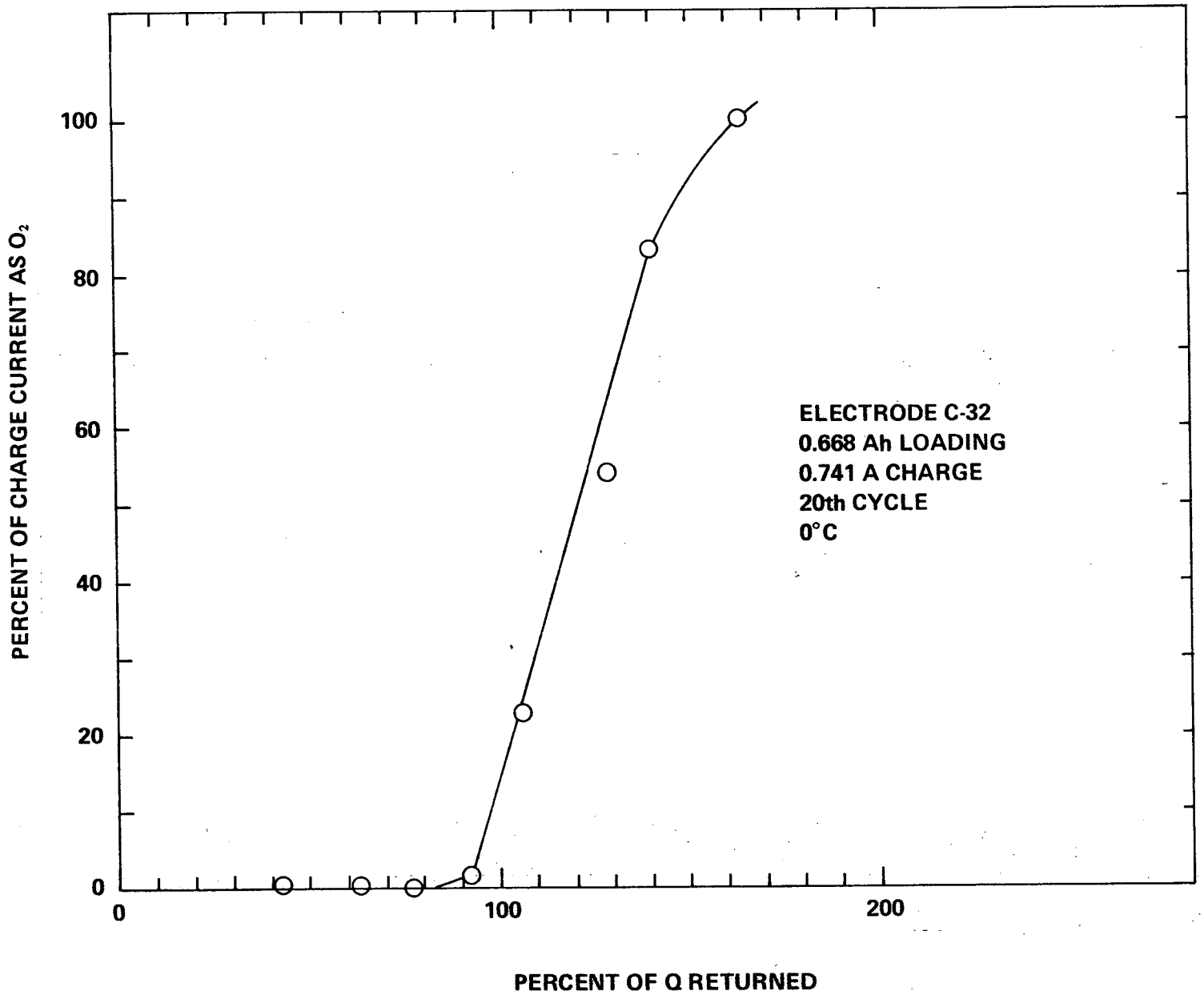

FIGURE 3. OXYGEN EVOLUTION ON CHARGE OF A HEAVILY LOADED NICKEL ELECTRODE

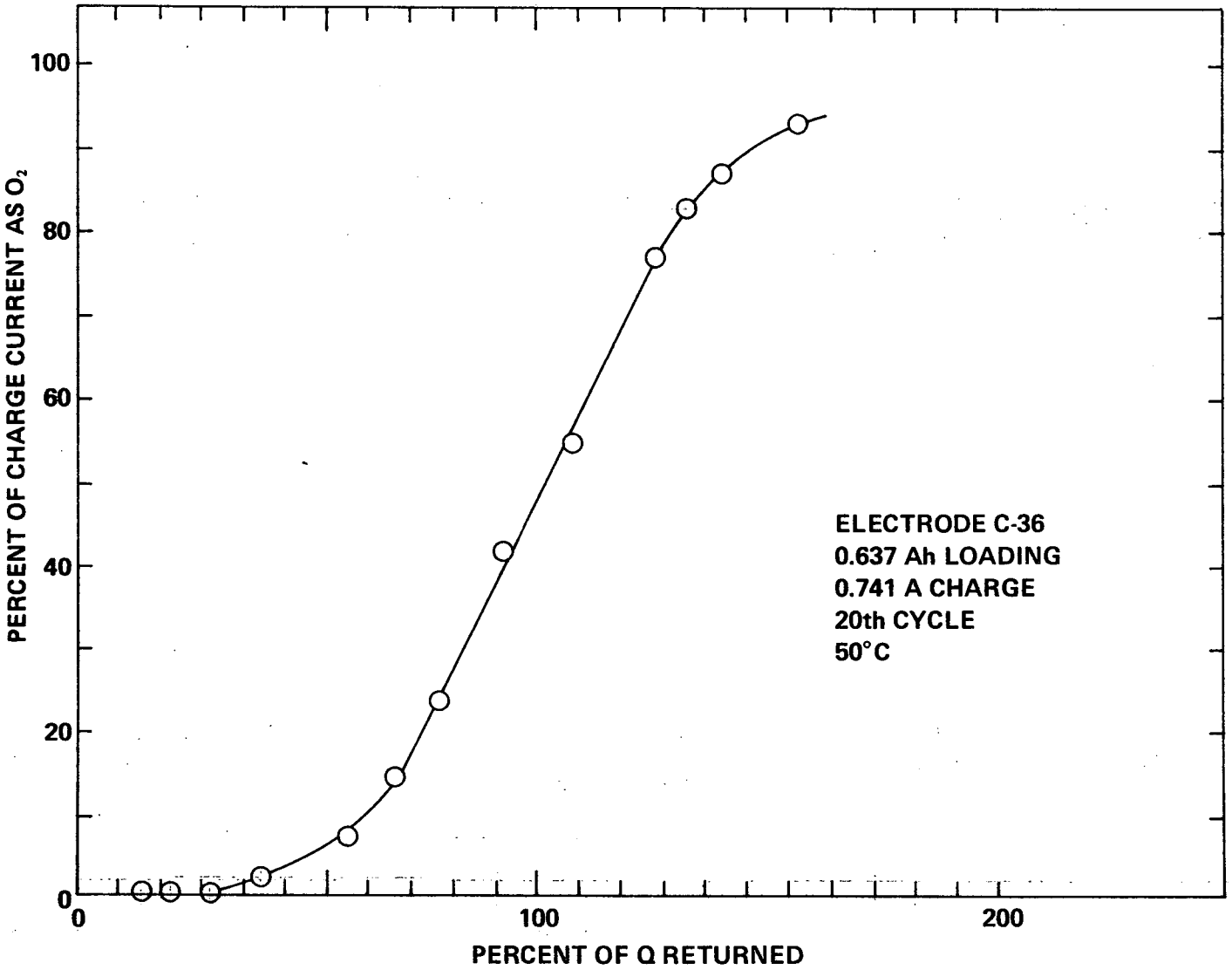

FIGURE 4. OXYGEN EVOLUTION ON CHARGE OF A HEAVILY LOADED NICKEL ELECTRODE

TABLE 2. ONSET OF OXYGEN EVOLUTION AT THIRD AND TWENTIETH CYCLE

EXP NO.	X_1	X_2	X_3	% Q_3	% Q_{20}
1	+	+	+	60	60
3	–	+	+	60	100
4	+	0	+	95	80
6	–	0	+	80	120
7	+	–	+	60	60
9	–	–	+	65	120
10	+	+	0	65	65*
12	–	+	0	90	90
13	+	0	0	100	100
15	–	0	0	90	120
16	+	–	0	130	70
18	–	–	0	90	130
19	+	+	–	75	70
21	–	+	–	120	120
22	+	0	–	75	75
24	–	0	–	100	100
25	+	–	–	60	70
27	–	–	–	85	100

* Data lost, estimated value

TABLE 3. MULTIPLIERS FOR CALCULATION OF EFFECTS & INTERACTIONS

EXP NO.	LINEAR X_1	LINEAR X_2	LINEAR X_3	QUAD X_1	QUAD X_2	QUAD X_3
1	+1	+1	+1	+1	+1	+1
2	0	+1	+1	−2	+1	+1
3	−1	+1	+1	+1	+1	+1
4	+1	0	+1	+1	−2	+1
5	0	0	+1	−2	−2	+1
6	−1	0	+1	+1	−2	+1
7	+1	−1	+1	+1	+1	+1
8	0	−1	+1	−2	+1	+1
9	−1	−1	+1	+1	+1	+1
10	+1	+1	0	+1	+1	−2
11	0	+1	0	−2	+1	−2
12	−1	+1	0	+1	+1	−2
13	+1	0	0	+1	−2	−2
14	0	0	0	−2	−2	−2
15	−1	0	0	+1	−2	−2
16	+1	−1	0	+1	+1	−2
17	0	−1	0	−2	+1	−2
18	−1	−1	0	+1	+1	−2
19	+1	+1	−1	+1	+1	+1
20	0	+1	−1	−2	+1	+1
21	−1	+1	−1	+1	+1	+1
22	+1	0	−1	+1	−2	+1
23	0	0	−1	−2	−2	+1
24	−1	0	−1	+1	−2	+1
25	+1	−1	−1	+1	+1	+1
26	0	−1	−1	−1	+1	+1
27	−1	−1	−1	+1	+1	+1

TABLE 4. EFFECTS OF VARIABLES AND INTERACTIONS ON THE "ONSET" OF O_2 EVOLUTIONS

	MAGNITUDE OF EFFECT ON	
VARIABLES (LINEAR)	% Q_3	% Q_{20}
Charge Temperature	– 5.0	–29.2
Charge Current	– 1.7	– 3.8
Loading $Ni(OH)_2$	– 7.9	0.4
Charge Temperature – Current	– 6.7	1.9
Charge Temperature – Loading	8.8	– 2.9
Charge Current – Loading	– 4.6	– 4.3
VARIABLES (QUADRATIC)		
Charge Current	–10.0	–14.3
Loading $Ni(OH)_2$	–16.3	– 6.3

The meaning of the signs of the effects of the variables in Table 4 is as follows:

1. A positive sign means an increase in the effect as the level of the variable is changed from the minus to the plus value. In the case at hand, oxygen is evolved at a high state of charge.

2. A negative sign means a decrease in the effect as the level of the variable is changed from the minus to the plus value. In this particular case, oxygen is evolved at a lower state of charge.

Thus it is seen from Table 4 that although all the effects have some degree of relevance as far as gassing of the nickel electrode on charge is concerned the biggest effect is the charge temperature. Oxygen evolution is observed at a 29.2 % lower state of charge at 50° C at the 20th cycle, than 0° C.

All the linear effects and interactions given in Table 4 are seen to be small in comparison with the magnitude with the temperature effect. Actually, the experimental error is in the 5-10% range so that of all the linear effects, only temperature is significant. It is when one looks at the quadratic effects, that the expected effects of charge current and $Ni(OH)_2$ loading manifest themselves with strong negative effects, indicating gassing at lower states of charge from the higher charge currents and the higher loadings. It is worthwhile to note the change in the effects caused by electrode cycling. It appears that the only effect that is altered by the cycling regime used in this study is the charge temperature. The effects of the other variables are changed to a lesser extent, some even in a favorable direction. The average of all the test conditions,

the average values of the data in Table 2, are for % Q_3 = 83.3, and % Q_{20} = 91.6. As a result, the aging if any, apparently improved the gassing properties of the electrodes, at least to a limited extent.

Perhaps a little different perspective of the data is offered in Figure 5 which shows the charge input at which the onset of gassing is observed as a function of loading at the three charge rates and the two temperatures studied. Here the data is given in a more natural form and one has a better feel for the experimental variation in the test data. Here also, it is apparent that there is a sizable effect of temperature, a smaller effect of loading.

2. Positive/Negative Capacity Ratio

It was stated previously that the primary objective of the positive electrode test program was to define an acceptable positive/negative active material ratio for the new negative limited cells, to assure minimum gassing operation on charge. On one hand, one wants to operate at the lowest state of charge of the positive electrode to eliminate gassing on charge and on the other hand, a low positive/negative ratio to achieve an attractive energy density. The positive/negative ratio and the positive electrode capacity at this stage in the program are important in order to select the appropriate hardware size to meet the cell delivery requirement in the program. The data already discussed provide the necessary input to choose a pos/neg ratio to assure minimum gassing, if one considers only the charge rate, charge temperature, and electrode loading. The worst conditions for gassing encountered were as mentioned earlier; the high charge rates, high temperature, and high loadings. It was decided to design around the toughest test variable which was found to be the charge temperature. The median loaded electrode, 20.5 g/in.^{3} $Ni(OH)_2$ loading was selected as being the most suitable from a consideration of their energy density, gassing, and physical properties. The lighter loaded electrode had somewhat better gassing properties but were too low in output. The test data for the suggested median loaded nickel electrodes at high and low temperatures are given in Figures 6 and 7, respectively, for the 0.247 A charge rate, the one corresponding closest to reality. It is apparent that these electrodes gas significantly at about 60% Q returned, so that the minimum positive/negative ratio would be 1.7:1. However, this should be considered, as only a first estimate; testing in cells corresponding closer to reality may reveal variables that must be considered in addition to the temperature, charge rate, and loading considerations made here.

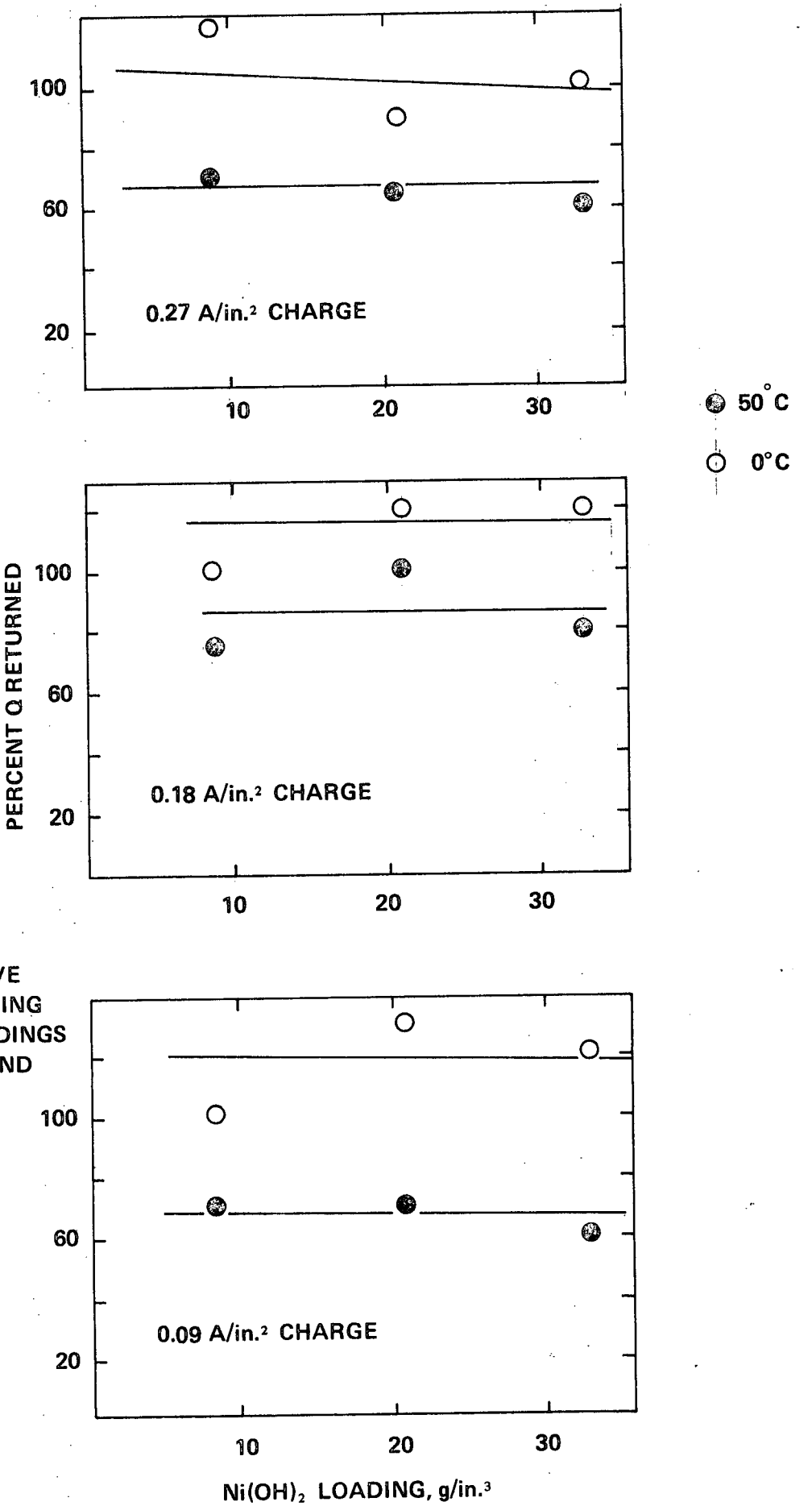

FIGURE 5. POSITIVE ELECTRODE GASSING AT VARIOUS LOADINGS CHARGE RATES AND TEMPERATURES

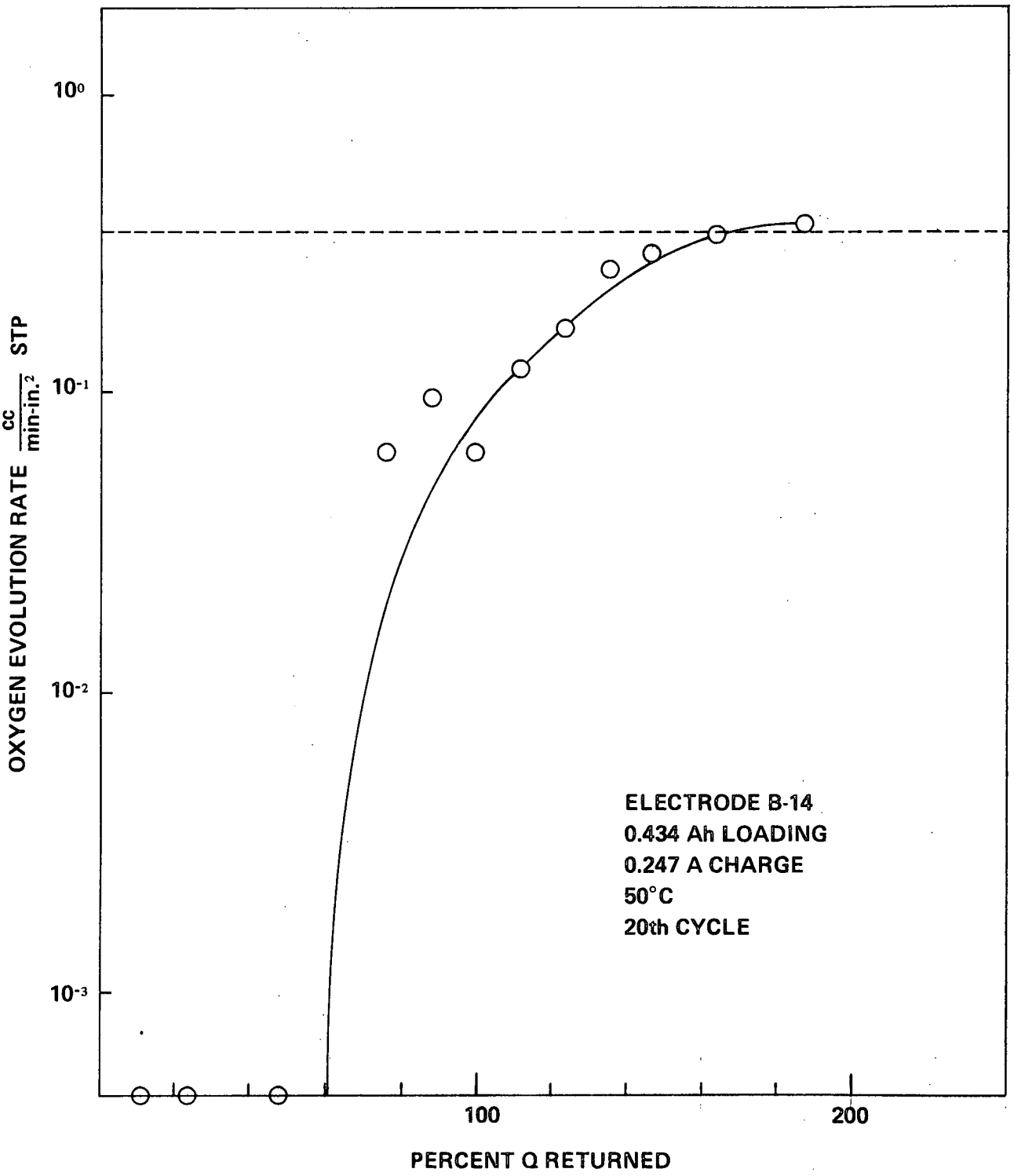

FIGURE 6. OXYGEN EVOLUTION ON CHARGE OF A MODERATELY LOADED NICKEL ELECTRODE AT THE WORST TEST VARIABLE, i.e., High Temperature

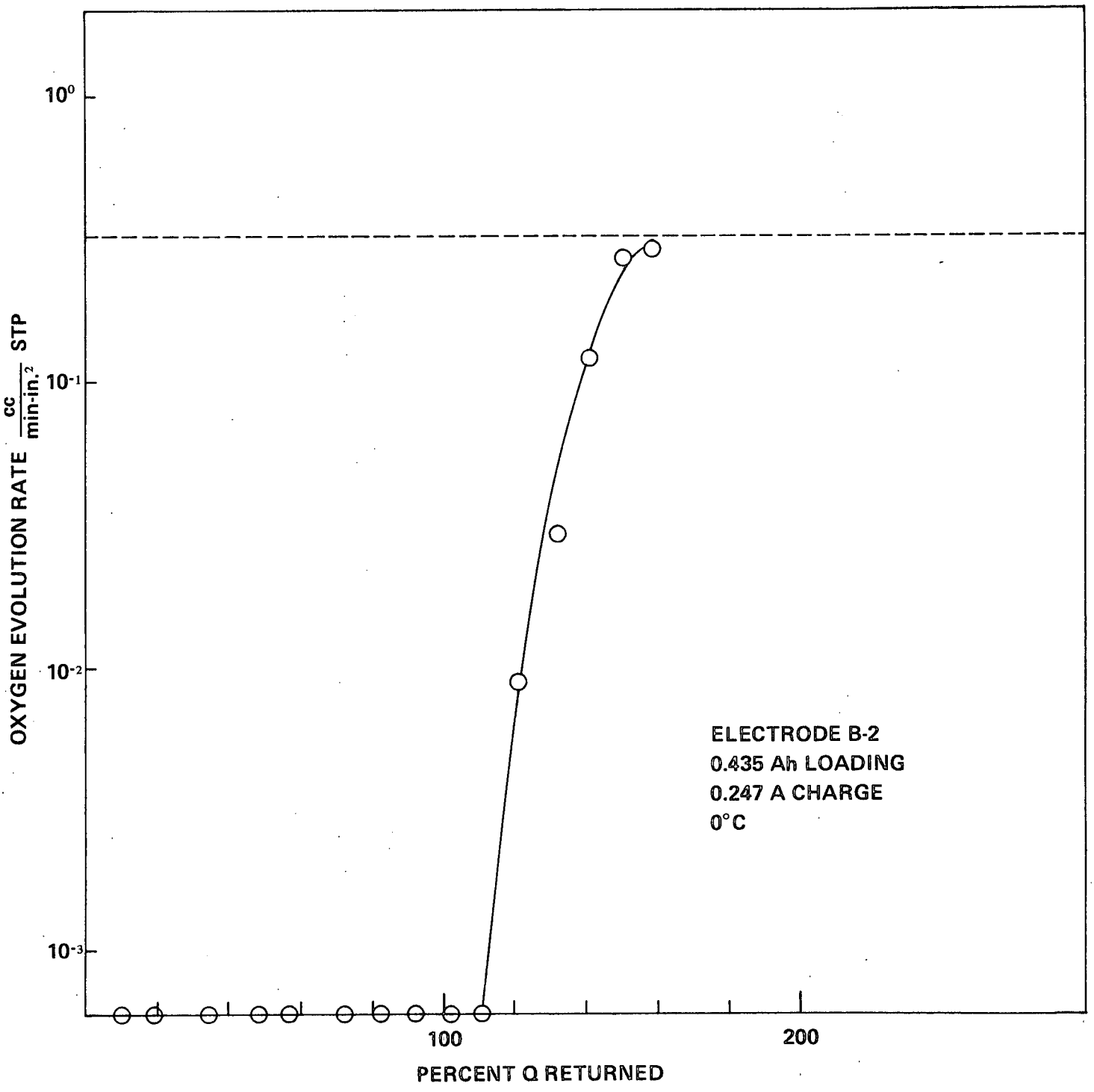

FIGURE 7. OXYGEN EVOLUTION ON CHARGE OF A MODERATELY LOADED NICKEL ELECTRODE AT LOW TEMPERATURE

IV. CONCLUSIONS

During the course of the second quarter of work on the development of a non-gassing nickel-cadmium battery, nickel electrodes were put through 20 cycles at 18 different test conditions, three loadings, three charge rates, and two temperatures. The gassing characteristics were determined as a function of charge input at the third and twentieth cycles for all the cells in order to establish the state-of-charge of the positive electrode at which they would possess acceptable gassing characteristics during charge. These data were then used to establish a minimum positive/negative ratio of 1.7:1. This value is of course based on charge rate, temperature, loading considerations only. Refinements on this value may have to be made as more data becomes available during the third quarter of the program, in the testing of more realistic cells.

In addition, an analysis of the above-mentioned data indicates that:

1. There was no overall deterioration of the gassing characteristics after the 20 cycles. Actually, the positive electrodes accepted charge better after 20 test cycles than earlier cycles. They actually gassed at higher states of charge at the end of 20 cycles. The effect of each variable changes with cycling, however.

2. The effect of temperature was found to be the single most important variable. Gassing at lower states-of-charge was enhanced at the high charge temperature. This variable was also shown to be age-dependent. Its magnitude changed from −5.0 at cycle 3 to −29.2 at cycle 20.

3. The $Ni(OH)_2$ loading was observed to have a large negative effect (−16.3) at the third cycle which indicates gassing at a lower state-of-charge. The magnitude of this effect decreased to −6.3% after 20 cycles.

4. The charge current exhibited no significant linear effects but showed a sizable negative quadratic effect on the electrode gassing, −10.0% at cycle 3 and −14.3% at cycle 20. The gassing characteristics were worse at the higher charge currents.

5. A nickel electrode with a loading in the range of 20 g/in.^{3} $Ni(OH)_2$ was selected as being most suitable for a nongassing cell from the point of view of their energy density, gassing, and physical properties.

Appendix A

Gassing Data For Nickel Electrodes

Table A-1

Gassing Data For Electrode C-36

0.637 AH Theo. Capacity, 741 ma Charge Rate, 50°C

Cycle #3

% Input	V_{O_2} cc/min	i_{O_2} (A)	$i_{O_2}/i \times 100$	% Returned Q
34.90	0.078	0.020	2.70	36.09
58.16	0.292	0.075	10.12	60.14
63.98	0.412	0.106	14.31	66.16
75.61	0.651	0.167	22.54	78.19
87.24	1.334	0.342	46.15	90.21
106.63	2.125	0.545	73.55	110.27
116.33	2.312	0.593	80.03	120.30
135.71	2.499	0.641	86.51	140.34
155.10	2.582	0.662	89.34	160.39

Cycle #20

11.63	0	0	0	10.86
23.27	0	0	0	21.74
34.90	0.009	0.002	0.27	32.60
46.53	0.077	0.019	2.56	43.46
58.16	0.169	0.043	5.80	54.32
69.80	0.354	0.089	12.01	65.19
81.43	0.591	0.149	20.11	76.06
96.94	1.053	0.266	35.90	90.54
116.33	1.397	0.352	47.50	108.65
135.71	1.957	0.494	66.67	126.76
145.41	2.102	0.530	71.53	135.82
155.10	2.231	0.563	75.98	144.87
174.49	2.386	0.602	81.24	162.98

Table A-2

Gassing Data For Electrode B-22

0.440 AH Theo. Capacity, 741 ma Charge Rate, 50°C

Cycle #3

% Input	V_{O_2} cc/Min	i_{O_2} (A)	$i_{O_2}/i \times 100$	% Returned
33.68	0.050	0.013	1.75	32.64
67.36	0.334	0.086	11.61	65.28
75.78	0.479	0.123	16.60	73.44
101.05	1.391	0.357	48.18	97.93
117.89	2.002	0.513	69.23	114.26
140.34	2.503	0.642	86.64	136.01
182.44	2.682	0.688	92.85	176.81

Cycle #20

Cell Shorted

Table A-3

Gassing Data For Electrode A-35
0.161 AH Theo. Capacity, 741 ma Charge Rate, 50°C

Cycle #3

% Input	V_{O_2} cc/min	i_{O_2} (A)	$i_{O_2}/i \times 100$	% Returned
23.01	0	0	0	24.86
46.02	0.082	0.021	2.83	49.73
69.04	0.270	0.069	9.31	74.60
115.06	1.466	0.376	50.74	124.33
161.09	2.215	0.568	76.65	174.06

Cycle #20

23.01	0	0	0	14.19
46.02	0	0	0	28.39
69.04	0	0	0	42.59
92.05	0.007	0.002	0.27	56.78
115.06	0.068	0.017	2.29	70.98
138.07	0.325	0.082	11.07	85.17
161.09	0.660	0.166	22.40	99.37
184.10	1.219	0.307	41.43	113.56
207.11	1.697	0.428	57.76	127.76
230.12	1.955	0.493	66.53	141.95
253.14	2.214	0.559	75.44	156.15

Table A-4

Gassing Data For Electrode C-35
0.634 AH Theo. Capacity, 414 ma Charge Rate, 50°C

Cycle #3

% Input	V_{O_2} cc/min	i_{O_2} (A)	$i_{O_2}/i \times 100$	% Ret'd.
27.71	0	0	0	30.16
43.53	0	0	0	48.25
54.42	0.021	0.005	1.21	60.32
65.30	0.038	0.010	2.42	72.38
76.18	0.083	0.021	5.07	84.44
92.51	0.186	0.048	11.59	102.54
103.39	0.445	0.114	27.54	114.60
114.27	0.860	0.221	53.38	126.66
119.72	0.831	0.214	51.69	132.70
141.48	1.084	0.278	67.15	156.82
152.37	1.121	0.288	69.57	168.89

Cycle #20

10.88	0	0	0	12.92
21.77	0	0	0	25.85
32.65	0	0	0	38.76
43.53	0.020	0.005	1.21	51.68
54.42	0.042	0.011	2.66	64.61
65.30	0.088	0.022	5.31	77.53
76.18	0.163	0.041	9.90	90.45
87.07	0.293	0.074	17.87	103.38
97.95	0.501	0.126	30.44	116.29
108.83	0.787	0.199	48.07	129.21
119.72	0.989	0.250	60.39	142.14
130.66	1.157	0.292	70.53	155.06
141.48	1.299	0.328	79.23	167.97
152.37	1.330	0.336	81.16	180.90
163.25	1.353	0.341	82.37	193.82

Table A-5

Gassing Data For Electrode B-19
0.443 AH Theo. Capacity, 414 ma Charge Rate, 50°C

Cycle #3

% Input	V_{O_2} cc/min	i_{O_2} (A)	$i_{O_2}/i \times 100$	% Ret'd.
23.36	0	0	0	24.47
46.73	0	0	0	48.94
70.09	0	0	0	73.40
85.67	0.033	0.008	1.93	89.72
101.24	0.204	0.053	12.80	106.03
140.18	1.069	0.275	66.43	146.81
155.76	1.161	0.298	71.98	163.13
186.91	1.099	0.282	68.12	195.75

Cycle #20

3.12	0	0	0	3.57
7.79	0	0	0	8.92
23.36	0	0	0	26.74
38.94	0	0	0	44.58
54.51	0.022	0.006	1.45	62.40
70.09	0.056	0.014	3.38	80.23
85.67	0.137	0.034	8.21	98.07
01.24	0.799	0.202	48.79	115.89
16.82	1.244	0.314	75.85	133.72
32.39	1.306	0.330	79.71	151.55
47.97	1.448	0.365	88.16	169.38
63.54	1.378	0.348	84.06	187.21
79.12	1.502	0.379	91.55	205.04
94.70	1.512	0.382	92.27	222.87

Table A-6

Gassing Data For Electrode A-8
0.176 AH Theo. Capacity, 414 ma Charge Rate, 50°C

Cycle #3

% Input	V_{O_2} cc/min	i_{O_2} (A)	$i_{O_2}/i \times 100$	% Ret'd.
7.84	0	0	0	6.54
19.60	0.008	0.002	0.48	16.35
39.20	0.008	0.002	0.48	32.70
137.22	1.001	0.256	61.84	114.46
294.03	1.007	0.259	62.56	245.26
450.85	1.498	0.385	93.00	376.07

Cycle #20

7.84	0	0	0	4.52
19.60	0	0	0	11.31
39.20	0	0	0	22.62
58.81	0	0	0	33.94
78.41	0	0	0	45.25
98.01	0.026	0.007	1.69	56.56
117.61	0.140	0.035	8.45	67.87
137.22	0.173	0.044	10.63	79.18
156.82	0.296	0.075	18.12	90.49
176.42	0.467	0.118	28.50	101.80
196.02	0.752	0.190	45.89	113.11
215.63	0.857	0.216	52.17	124.43
254.83	1.013	0.256	61.84	147.05

Table A-7

Gassing Data For Electrode C-14
0.645 AH Theo. Capacity, 247 ma Charge Rate, 50°C

Cycle #3

% Input	V_{O_2} cc/min	i_{O_2} (A)	$i_{O_2}/i \times 100$	% Returned
19.15	0	0	0	33.66
28.72	0.020	0.005	2.02	50.48
38.29	0.085	0.022	8.91	67.29
47.87	0.171	0.044	17.81	84.13
51.06	0.195	0.050	20.24	89.74
57.44	0.255	0.065	26.32	100.95
63.82	0.327	0.084	34.01	112.16
70.21	0.392	0.100	40.49	123.39
76.59	0.472	0.121	48.99	134.61
82.97	0.532	0.136	55.06	145.82
95.74	0.641	0.164	66.40	168.26
108.50	0.707	0.181	73.28	190.69
114.88	0.720	0.185	74.90	201.90
121.27	0.806	0.206	83.40	213.30

Cycle #20

19.15	0	0	0	32.94
31.91	0.025	0.006	2.43	54.89
38.29	0.053	0.014	5.67	65.86
51.06	0.147	0.037	14.98	87.87
57.44	0.182	0.046	18.62	98.80
63.82	0.192	0.049	19.84	109.77
70.21	0.239	0.060	24.29	120.76
76.59	0.259	0.066	26.72	131.74
82.97	0.304	0.077	31.17	142.71
95.74	0.369	0.093	37.65	164.67
108.50	0.441	0.112	45.34	186.62
114.88	0.502	0.127	51.42	197.59
121.27	0.528	0.134	54.25	208.58

Table A-8

Gassing Data For Electrode B-14

0.434 AH Theo. Capacity, 247 ma Charge Rate, 50°C

Cycle #3

% Input	V_{O_2} cc/min	i_{O_2} (A)	$i_{O_2}/i \times 100$	% Returned
9.49	0	0	0	20.91
18.97	0	0	0	41.79
37.94	0.012	0.003	1.22	83.58
52.17	0.055	0.014	5.67	114.93
61.66	0.108	0.028	11.34	135.84
80.63	0.209	0.054	21.86	177.63
90.11	0.333	0.085	34.41	198.52
99.60	0.482	0.123	49.80	219.42
109.08	0.792	0.203	82.19	240.31
118.57	0.639	0.164	66.40	261.22
132.80	0.711	0.182	73.68	292.56
151.77	0.893	0.229	92.71	334.36

Cycle #20

9.49	0	0	0	11.77
18.97	0	0	0	23.52
37.94	0	0	0	47.05
61.66	0.161	0.041	16.60	76.46
71.14	0.243	0.061	24.70	88.21
80.63	0.167	0.042	17.00	99.98
90.11	0.307	0.078	31.58	111.74
99.60	0.431	0.109	44.13	123.50
109.08	0.691	0.175	70.85	135.26
118.57	0.773	0.196	79.35	147.03
132.80	0.887	0.225	91.09	164.67
151.77	0.961	0.243	98.38	188.20

Table A-9

Gassing Data For Electrode A-4

0.165 AH Theo. Capacity, 247 ma Charge Rate, 50°C

Cycle #3

% Input	V_{O_2} cc/min	i_{O_2} (A)	$i_{O_2}/i \times 100$	% Returned
4.99	0	0	0	4.71
12.47	0	0	0	11.76
37.42	0.017	0.004	1.62	35.28
62.37	0.107	0.027	10.93	58.81
87.32	0.339	0.087	35.22	82.33
124.75	0.666	0.171	69.23	117.62
174.65	0.586	0.150	60.73	164.67
336.82	0.830	0.213	86.24	317.57

Cycle #20

4.99	0	0	0	3.47
12.47	0	0	0	8.68
37.42	0	0	0	26.05
62.37	0	0	0	43.42
87.32	0.069	0.018	7.29	60.79
112.27	0.123	0.031	12.55	78.16
137.22	0.103	0.026	10.53	95.53
174.65	0.372	0.094	38.06	121.59
361.77	0.906	0.230	93.12	251.87

Table A-10

Gassing Data For Electrode C-32

0.668 AH Theo. Capacity, 741 ma Charge Rate, 0°C

Cycle #3

% Input	V_{O_2} cc/min	i_{O_2} (A)	$i_{O_2}/i \times 100$	% Returned
33.28	0	0	0	42.03
49.92	0.068	0.017	2.29	63.04
61.01	0.658	0.165	22.27	77.04
72.10	1.380	0.347	46.83	91.05
83.20	1.851	0.465	62.75	105.06
101.68	2.297	0.578	78.00	128.40
110.93	2.395	0.602	81.24	140.08
129.42	2.502	0.629	84.89	163.43

Cycle #20

33.28	0	0	0	42.03
49.92	0	0	0	63.04
61.01	0	0	0	77.04
72.10	0.043	0.011	1.49	91.05
83.20	0.595	0.150	20.24	105.06
101.68	1.410	0.356	48.04	128.40
110.93	2.153	0.544	73.41	140.08
129.42	2.587	0.654	88.26	163.43

Table A-11

Gassing Data For Electrode B-32
0.450 AH Theo. Capacity, 741 ma Charge Rate, 0°C

Cycle #3

% Input	V_{O_2} cc/min	i_{O_2} (A)	$i_{O_2}/i \times 100$	% Ret'd.
32.93	0	0	0	31.87
57.63	0	0	0	55.77
82.33	0.027	0.007	0.95	79.67
98.80	0.497	0.125	16.87	95.61
115.27	1.757	0.442	59.65	111.55
137.22	2.554	0.642	86.64	132.79

Cycle #20

32.93	0	0	0	31.87
57.63	0	0	0	55.77
82.33	0.170	0.043	5.80	79.67
98.80	0.431	0.109	14.71	95.61
115.27	1.751	0.443	59.78	111.55
137.22	2.837	0.717	96.76	132.79

Table A-12

Gassing Data For Electrode A-50
0.162 AH Theo. Capacity, 741 ma Charge Rate, 0°C

Cycle #3

% Input	V_{O_2} cc/min	i_{O_2} (A)	$i_{O_2}/i \times 100$	% Returned
22.87	0.003	0.001	0.14	34.40
45.74	0.003	0.001	0.14	62.80
68.61	0.004	0.001	0.14	94.19
114.35	2.397	0.603	81.38	156.99
182.96	2.907	0.731	98.65	251.18

Cycle #20

22.87	0	0	0	31.40
45.74	0	0	0	62.80
68.61	0.013	0.003	0.41	94.19
114.35	1.987	0.502	67.75	156.99
182.96	2.935	0.742	100.14	251.18

Table A-13

Gassing Data For Electrode C-31
0.658 AH Theo. Capacity, 414 ma Charge Rate, 0°C

Cycle #3

% Input	V_{O_2} cc/min	i_{O_2} (A)	$i_{O_2}/i \times 100$	% Returned
20.97	0	0	0	25.55
41.95	0	0	0	51.12
62.92	0.047	0.012	2.90	76.67
73.40	0.342	0.086	20.77	89.44
83.89	0.863	0.217	52.42	102.22
94.38	1.014	0.255	61.59	115.00
99.62	1.117	0.280	67.63	121.39
115.35	1.149	0.289	69.81	140.56
136.32	0.986	0.248	59.90	166.11

Cycle #20

36.70	0.006	0.001	0.24	44.23
41.95	0.004	0.001	0.24	50.56
62.92	0	0	0	75.83
73.40	0	0	0	88.46
83.89	0	0	0	101.10
94.38	0.083	0.021	5.07	113.74
99.62	0.163	0.041	9.90	120.06
110.11	0.638	0.161	38.89	132.70
115.35	1.054	0.266	64.25	139.01
136.32	1.441	0.363	87.68	164.28

Table A-14

Gassing Data For Electrode B-12

0.442 AH Theo. Capacity, 414 ma Charge Rate, 0°C

Cycle #3

% Input	V_{O_2} cc/min	i_{O_2} (A)	$i_{O_2}/i \times 100$	% Returned
15.61	0	0	0	15.16
39.03	0	0	0	37.92
70.25	0	0	0	68.24
35.86	0.109	0.027	6.52	83.41
101.47	0.655	0.165	39.86	98.57
117.08	1.158	0.291	70.29	113.74
132.69	1.335	0.335	80.92	128.90
156.11	1.310	0.329	79.47	151.65
187.33	1.590	0.399	96.38	181.98

Cycle #20

15.61	0.008	0.002	0.48	17.34
39.03	0.006	0.001	0.24	43.35
70.25	0	0	0	78.02
85.86	0.010	0.003	0.73	95.35
101.47	0.107	0.027	6.52	112.69
117.08	0.489	0.123	29.71	130.02
132.69	1.312	0.331	79.95	147.36
156.11	1.477	0.372	89.86	173.37
187.33	1.694	0.427	103.14	208.04

Table A-15

Gassing Data For Electrode A-34
0.162 AH Theo. Capacity, 414 ma Charge Rate, 0°C

Cycle #3

% Input	V_{O_2} cc/min	i_{O_2} (A)	i_{O_2} x 100	% Returned
8.52	0	0	0	12.11
21.30	0	0	0	30.27
63.89	0	0	0	90.79
127.78	1.460	0.367	88.65	181.58
149.07	1.581	0.397	95.89	211.84
212.96	1.564	0.393	94.93	302.63

Cycle #20

8.52	0.012	0.003	0.73	12.11
21.30	0.012	0.003	0.73	30.27
63.89	0.049	0.012	2.90	90.79
85.19	0.828	0.209	50.48	121.06
127.78	1.473	0.371	89.61	181.58
212.96	1.614	0.407	98.31	302.63

Table A-16

Gassing Data For Electrode C-26
0.663 AH Theo. Capacity, 247 ma Charge Rate, 0°C

Electrode C-26

Cycle #1

% Input	V_{O_2} cc/min	i_{O_2} (A)	$i_{O_2}/i \times 100$ (%)
15.52	0.010	0.003	1.22
24.84	0.060	0.015	6.07
43.46	0.380	0.095	38.46
62.09	0.581	0.145	58.71
74.51	0.687	0.171	69.23
90.03	0.711	0.177	71.66
105.56	0.841	0.209	84.62
121.08	0.780	0.194	78.54
130.39	0.824	0.205	83.00
139.71	0.902	0.225	91.09
149.02	0.775	0.193	78.14
152.12	0.912	0.227	91.90

Cycle #3

% Input	V_{O_2} cc/min	i_{O_2} (A)	$i_{O_2}/i \times 100$ (%)
15.52	0.010	0.003	1.22
24.84	0.060	0.015	6.07
43.46	0.380	0.095	38.46
62.09	0.581	0.145	58.71
74.51	0.687	0.171	69.23
90.03	0.711	0.177	71.66
105.56	0.841	0.209	84.62
121.08	0.780	0.194	78.54
130.39	0.824	0.205	83.00
139.71	0.902	0.225	91.09
149.02	0.775	0.193	78.14
152.12	0.912	0.227	91.90

Cycle #20

% Input	V_{O_2}	i_{O_2}	$i_{O_2}/i \times 100$	% Returned
15.52	0	0	0	24.21
40.36	0	0	0	62.96
49.67	0	0	0	77.49
55.88	0	0	0	87.17
62.09	0	0	0	96.86
68.30	0.009	0.002	0.81	106.55
74.51	0.067	0.017	6.88	116.24
80.72	0.172	0.043	17.41	125.92
86.93	0.336	0.085	34.41	135.61
93.14	0.495	0.125	50.61	145.30
99.35	0.652	0.164	66.40	154.99
111.76	0.814	0.205	83.00	174.35

Table A-17

Gassing Data for Electrode B-2

0.435 AH Theo. Capacity, 247 ma Charge Rate, 0°C

Cycle 1

% Chg. Input	V_{O_2} cc/min	i_{O_2} (A)	$i_{O_2}/i \times 100$ (%)	% Ret'd.
9.46	0	0	0	
18.93	0	0	0	
33.12	0	0	0	
47.32	0	0	0	
61.51	0.013	0.003	1.22	
85.17	0.400	0.100	40.49	
104.10	0.651	0.162	65.59	
127.76	0.628	0.156	63.16	
141.95	0.760	0.189	76.52	
146.69	0.694	0.173	70.04	
170.35	0.759	0.189	76.52	

Cycle #3

% Input	V_{O_2} cc/min	i_{O_2} (A)	$i_{O_2}/i \times 100$ (%)	% Returned
9.46	0	0	0	9.62
18.93	0	0	0	19.24
33.12	0	0	0	33.66
47.32	0	0	0	48.09
56.78	0	0	0	57.71
70.98	0.010	0.003	1.22	72.14
80.44	0.034	0.009	3.64	81.76
89.90	0.342	0.086	34.82	91.37
99.37	0.618	0.156	63.16	101.00
108.83	0.752	0.190	76.92	110.61
132.49	0.743	0.188	76.11	134.66
156.15	0.836	0.211	85.43	158.70

Table A-17 Continued

Cycle 20

% Chg. Input	V_{O_2} cc/min	i_{O_2} (A)	$i_{O_2}/i \times 100$ (%)	% Ret'd.
9.46	0	0	0	9.62
18.93	0	0	0	19.24
33.12	0	0	0	33.66
47.32	0	0	0	48.09
56.78	0	0	0	57.71
70.98	0	0	0	72.14
80.44	0	0	0	81.76
89.90	0	0	0	91.37
99.37	0	0	0	101.00
108.83	0	0	0	110.61
118.30	0.023	0.006	2.43	120.24
127.76	0.078	0.020	8.10	129.85
137.22	0.312	0.079	31.98	139.46
146.69	0.682	0.172	69.64	149.09
156.15	0.772	0.195	78.95	158.70

Table A-18

Gassing Data For Electrode A-30
0.162 AH Theo. Capacity, 247 ma Charge Rate, 0°C

Cycle #1

% Chg. In (Theo.)	V_{O_2} cc/min	i_{O_2} (A)	$i_{O_2}/i \times 100$	% Ret'd.
12.71	0	0	0	
38.12	0	0	0	
76.24	0	0	0	
114.35	0.289	0.072	29.15%	
139.76	0.464	0.116	46.96	
152.47	0.589	0.147	59.51	
190.59	0.707	0.176	71.26	
266.82	0.787	0.196	79.35	
319.64	0.819	0.204	82.59	

Cycle #3

% Chg. Input	V_{O_2} cc/min	i_{O_2} (A)	$i_{O_2}/i \times 100$ (%)	% Returned
5.08	0	0	0	6.38
12.71	0	0	0	15.96
38.12	0	0	0	47.87
76.24	0.750	0.190	76.92	95.74
101.65	0.806	0.204	82.59	126.65
114.35	0.940	0.238	96.36	143.60
139.76	0.927	0.235	95.14	175.51
177.88	0.986	0.249	100.81	223.38
330.35	0.889	0.225	91.09	414.86

Table A-18 Continued

Cycle 20

% Chg. Input	V_{O_2} cc/min	i_{O_2} (A)	$i_{O_2}/i \times 100$ (%)	% Ret'd.
5.08	0	0	0	6.38
12.71	0	0	0	15.96
38.12	0	0	0	47.87
76.23	0.043	0.011	4.45	95.73
101.65	0.773	0.195	78.95	127.65
114.35	0.856	0.216	87.45	143.60
139.76	0.979	0.247	100.00	175.51
177.88	0.973	0.246	99.60	223.38